RESEARCH ARTICLE OPEN ACCESS

Immuno-Proteomic Features Associated to Relapse Risk in Myelin Oligodendrocyte Glycoprotein Antibody-Associated Disease

Gerardina Gallaccio,[1,2,3,*] Anna Müller,[1,2,3,*] Meng Wang,[1,2,3] Lisa-Marie Diekmann,[1,2,3] Carolin Otto,[4] Alessandro Dinoto,[5] Vanessa Chiodega,[5] Carolin Schwake,[6] Sven Jarius,[7] Tatiana Usnich,[8] Pia Sophie Sperber,[4] Lina Anderhalten,[8] Tatchaporn Ongphichetmetha,[9] Angus Byars,[10] Deni Subasic,[10] Desiree Kunkel,[11] Ilya Ayzenberg,[6] Sara Mariotto,[5] Sara Samadzadeh,[1,2,3,†] Friedemann Paul,[1,2,3,4,8,†] and Chotima Böttcher[1,2,3,†]

Correspondence
Dr. Böttcher
chotima.boettcher@charite.de

Neurol Neuroimmunol Neuroinflamm 2026;13:e200615. doi:10.1212/NXI.0000000000200615

Abstract

Background and Objectives

Myelin oligodendrocyte glycoprotein antibody-associated disease (MOGAD) is an inflammatory demyelinating disorder that overlaps clinically with multiple sclerosis (MS) but immunopathologically distinct. Although often considered an acute inflammatory disease, recurrent attacks in MOGAD can lead to demyelination, axonal injury, and secondary neurodegeneration. Reliable biomarkers associated with relapse risk and disease subphenotypes, including optic neuritis, remain limited. Here, we aimed to define molecular and cellular signatures that distinguish MOGAD from MS as a prototypical neuroinflammatory disease and from Alzheimer disease (AD) as a proxy of neurodegeneration and to identify candidate immune–proteomic features associated with relapse frequency and clinical phenotype in MOGAD.

Methods

CSF, serum, and whole-blood samples from patients with MOGAD (n = 67), MS (n = 49), and AD (n = 36) were profiled using NULISAseq™ CSF proteomics, Olink Explore 3072 CSF and serum proteomics, and high-dimensional mass cytometry for immune cell characterization. In MOGAD, longitudinal clinical data, including total attack counts from the earliest documented attack through follow-up, were integrated with immune and proteomic profiles to assess associations with disease course and clinical phenotype.

Results

CSF and blood proteomic profiling revealed distinct inflammatory and cardiometabolic proteomic profiles in MOGAD, differentiating it from both MS and AD. Compared with MS, MOGAD showed relative reductions in lymphocyte populations with regulatory phenotypes. Within MOGAD, relapsing disease was associated with reduced frequencies of $CD8^+CCR7^+CD31^+CTLA4^+$ T cells and concurrent expansion of double-negative γδ T-cell subsets. IL-13 correlated positively with relapse frequency and inversely with circulating regulatory T cells, whereas IL-32 and CASP4 showed opposite associations, correlating negatively with relapse count and positively with Treg frequency. IL-13 was also inversely associated with CD31-expressing $CD8^+$ T cells. Phenotype-stratified analyses suggested that these immune-proteomic relationships differed according to clinical presentation, including optic neuritis vs nonoptic neuritis phenotypes.

MORE ONLINE

Supplementary Material

*These authors contributed equally to this work.

†These authors jointly directed this work.

[1]Experimental and Clinical Research Center, a cooperation between the Max Delbrück Center for Molecular Medicine in the Helmholtz Association and Charité Universitätsmedizin Berlin, Germany; [2]Charité—Universitätsmedizin Berlin, corporate member of Freie Universität Berlin and Humboldt-Universität zu Berlin, Germany; [3]Max Delbrück Center for Molecular Medicine in the Helmholtz Association (MDC), Berlin, Germany; [4]Department of Neurology with Experimental Neurology, Charité—Universitätsmedizin Berlin, corporate member of Freie Universität Berlin and Humboldt-Universität zu Berlin, Germany; [5]Neurology Unit, Department of Neurosciences, Biomedicine and Movement Sciences, University of Verona, Italy; [6]Department of Neurology, St. Josef Hospital, Ruhr University Bochum, Germany; [7]Division of Neuroimmunology, Department of Neurology, University of Heidelberg, Germany; [8]Neuroscience Clinical Research Center, Charité—Universitätsmedizin Berlin, corporate member of Freie Universität Berlin and Humboldt-Universität zu Berlin, Germany; [9]Siriraj Neuroimmunology Center, Faculty of Medicine Siriraj Hospital, Mahidol University, Bangkok, Thailand; [10]F. Hoffmann-La Roche Ltd. (A.B., D.S.), Basel, Switzerland; and [11]Flow & Mass Cytometry Core Facility, Berlin Institute of Health at Charité - Universitätsmedizin Berlin, Germany.

The Article Processing Charge was funded by the authors.

Glossary

AD = Alzheimer disease; **AQP4-NMOSD** = aquaporin-4 antibody–positive neuromyelitis optica spectrum disorder; **DEP** = differentially expressed protein; **FDR** = false discovery rate; **IDD** = inflammatory demyelinating disease; **MOGAD** = myelin oligodendrocyte glycoprotein antibody-associated disease; **MS** = multiple sclerosis; **NULISA** = nucleic acid–linked immunosandwich assay; **QC** = quality control; **RTE** = recent thymic emigrant; **WB** = whole blood.

Discussion

This integrative immune-proteomic analysis identifies cellular and molecular features associated with relapsing vs monophasic MOGAD, suggesting a model of impaired peripheral immune regulation in relapsing disease. While exploratory, these findings generate a concrete hypothesis for future longitudinal and functional studies aimed at refining biomarker-based monitoring and informing individualized therapeutic strategies in MOGAD.

Introduction

Inflammatory demyelinating diseases (IDDs) of the CNS include multiple sclerosis (MS), aquaporin-4 antibody–positive neuromyelitis optica spectrum disorder (AQP4-NMOSD), and myelin oligodendrocyte glycoprotein antibody–associated disease (MOGAD). While MS is characterized by heterogeneous, T-cell–driven autoimmunity with variable B-cell involvement, and AQP4-NMOSD is mediated by astrocyte-directed autoantibodies, MOGAD represents a distinct disease entity defined by core clinical syndromes and antibodies targeting conformational epitopes of MOG.[1-4]

Clinically, MOGAD most often presents with optic neuritis, myelitis, or acute disseminated encephalomyelitis. Although long-term disability is less frequent than in MS, relapses can be severe, and a relapsing disease course occurs in approximately 30%–60% of adults.[5-7] Identifying patients at risk of relapse is therefore critical for guiding long-term immunotherapy decisions.[6,8] However, reliable biomarkers of relapse risk remain lacking. Imaging and CSF analyses poorly distinguish disease course, and serum neurofilament light chain reflects recent injury rather than future relapse risk.[9,10] Persistence of MOG-IgG seropositivity is the most consistent predictor, yet it is imperfect, as some seropositive patients remain monophasic and relapses may occur after seronegative conversion,[1,11,12] indicating additional immunologic modifiers of disease course.

MOG-IgG mediates CNS injury via complement-dependent cytotoxicity, antibody-dependent cellular cytotoxicity, and phagocytosis, with effector activity particularly elevated during relapses.[13] Beyond humoral mechanisms, recent studies have identified expansion of cytotoxic lymphocytes, inflammatory monocytes, and IL-17–associated pathways, alongside fluctuating cytokine profiles and elevated BAFF levels.[14-17] Single-cell analyses further reveal increased cytotoxic immune populations with reduced memory B-cell signatures.[16]

Despite these advances, immune profiling has not yet enabled robust relapse stratification. In particular, the contribution of regulatory immune populations remains insufficiently understood. Relapsing disease is more common in adults, suggesting age-dependent changes in immune regulation. Recent thymic emigrants (RTEs), which decline with age, contribute to peripheral tolerance and Treg homeostasis and may influence inflammatory control during immune challenges.[18,19]

In this study, we applied high-dimensional immune and proteomic profiling of CSF and blood from patients with MOGAD, MS, and Alzheimer disease (AD) using mass cytometry and proximity-based proteomics. We aimed to define molecular and cellular signatures distinguishing MOGAD from neuroinflammatory and neurodegenerative comparators and to identify immune-proteomic features associated with relapse frequency and disease course in MOGAD.

Methods

Standard Protocol Approvals, Registrations, and Patient Consents

This study was approved by the Ethics Committee of Charité–Universitätsmedizin Berlin, University of Verona and Ruhr University Bochum (EA1/386/20 and EA1/362/20) and conducted in accordance with the Declaration of Helsinki (1964 and amendments). Written informed consent was obtained from all participants; no financial compensation was provided.

Study Design

Patients with MOGAD (n = 67) and non-MOGAD neurologic controls, including MS (n = 49) and AD (n = 36), were recruited from 3 centers: Charité–Universitätsmedizin Berlin (MOGAD, MS and AD patients), University of Verona (MOGAD only), and Ruhr University Bochum (MOGAD only). CSF and peripheral blood (serum and whole blood) samples were collected. Patients with MOGAD were diagnosed according to the recently published International MOGAD Panel criteria by Banwell et al.,[1] MS was diagnosed based on the 2017 McDonald criteria, and AD cases fulfilled the ATN classification (A = Amyloid pathology; T = tau

pathology, N = neurodegeneration/neuronal injury) and are $A^+T^+N^+$. Specifically, for defining the Aβ and tau pathologies, reduced CSF amyloid-β42 concentrations or positive amyloid PET scans indicate the presence of amyloid pathology (A), while elevated CSF phosphorylated tau (primarily p-tau181) or tau PET imaging reflects the presence of insoluble tau fibrils (T).[20]

To characterize the molecular and cellular features underlying MOGAD pathology and to identify soluble biomarkers distinguishing it from inflammation driven by autoimmunity, as in MS, and neurodegeneration-associated neuroinflammation, as in AD, we conducted integrative analyses of CSF and blood samples obtained from 3 independent data centers.

For all paired samples, CSF and blood were collected from the same individual on the same day. In patients sampled during an acute attack, both biofluids were obtained within 30 days of symptom onset and before initiation of any acute immunotherapy (e.g., corticosteroids, IVIG, or plasma exchange). In total, the study included samples from 67 with MOGAD, 49 with MS, and 36 with AD (Figure 1, eTable 1). Using targeted proteomics and high-dimensional cell profiling technologies, we generated comprehensive molecular and cellular profiles from CSF, whole blood (WB), and serum samples. Targeted proteomic profiling of CSF was first performed using the nucleic acid–linked immuno-sandwich assay (NULISA) platform in a subset of individuals (MOGAD: n = 21; MS: n = 22; AD: n = 36). To obtain deeper coverage of protein networks and biological pathways, Olink proteomics was subsequently applied to CSF (MOGAD: n = 13; MS: n = 28) and serum (MOGAD: n = 64; MS: n = 16) samples. Immune cell populations in whole blood were characterized by high-dimensional mass cytometry (CyTOF) (MOGAD: n = 22; MS: n = 16). To explore clinical correlates of molecular signatures, we focused on the MOGAD cohort and examined associations between differentially expressed proteins (DEPs) and clinical parameters, including disease duration and relapse frequency. Patient stratification into monophasic vs relapsing MOGAD was based solely on clinical course, independent of molecular or cellular measurements.

Proteomic Analyses

NULISA (CSF, MOGAD vs MS, and MOGAD vs AD)

CSF from MOGAD (n = 21), MS (n = 22) and AD (n = 36) was analyzed with the NULISAseq™ platform (Alamar). The CNS Disease 120-plex and Inflammation 250-plex panels were applied. Protein concentrations were normalized to internal and inter-plate controls, $\log_2$-transformed to NULISA Protein Quantification (NPQ), and analyzed by linear mixed-effects modeling (limma V3.58.1; age as covariate, Benjamini-Hochberg false discovery rate (FDR) < 0.05).[21] Proteins with detection rates below 80% across samples were excluded during the initial quality control filtering before downstream analyses.

Figure 1 Schematic Overview of the Experimental Workflow

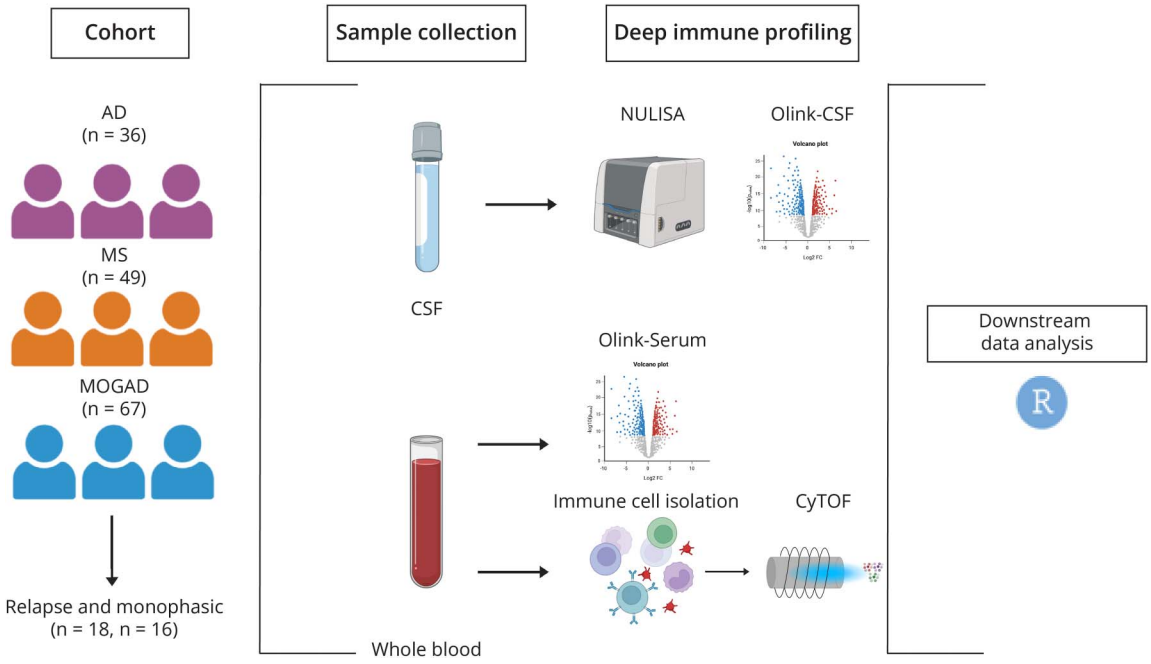

The study cohort included CSF and whole blood samples collected from patients with Alzheimer disease (AD, n = 36), multiple sclerosis (MS, n = 49), and myelin oligodendrocyte glycoprotein antibody–associated disease (MOGAD, n = 67), together with their corresponding clinical parameters. Samples were recruited from 3 independent data centers. CSF samples were analyzed using targeted proteomics with the NULISA™ platform and the Olink Explore 3072 panel. Serum samples were profiled using Olink Explore, while immune cells isolated from whole blood were characterized by high-dimensional cytometry (CyTOF) using 3 distinct antibody panels.

Olink (CSF and Serum, MOGAD vs MS)

CSF from MOGAD (n = 13) and MS (n = 49) and serum from MOGAD (n = 64) and MS (n = 16) were analyzed using Olink Explore 3072, covering 8 panels targeting >3,000 proteins. Normalized protein expression (NPX) values were calculated after quality control (QC), $\log_2$-transformed, and analyzed using the OlinkAnalyze R package (v4.0.1).[22] DEPs were identified by limma (age as covariate, BH-FDR <0.05), with 508 DEPs detected in serum. Proteins with detection rates below 80% across samples were excluded during the initial quality control filtering before downstream analyses.

Immune Cell Profiling by Mass Cytometry

Whole blood was collected in EDTA tubes, maintained at 4°C, and processed within 30 minutes of venipuncture. Samples were fixed using SmartTube Proteomic Stabilizer and stored at −80°C until analysis, as previously described.[23] Three antibody panels were used: panel A (T and NK cells), panel B (B cells and myeloid populations), and panel C (neutrophils). Antibodies were either preconjugated (Standard BioTools) or labeled in-house using the MaxPar X8 kit.

Fixed samples were thawed, barcoded using 6 palladium isotopes (Cell-ID 20-Plex Pd kit; 6-choose-3 scheme), pooled, and stained for surface and/or intracellular markers. Surface staining was performed at 4°C, followed by fixation; intracellular staining was performed after permeabilization at room temperature. Cells were labeled with iridium intercalator for DNA staining before acquisition. Data were processed, as described previously.[23,24] Intact single cells were gated using DNA and event length. After debarcoding, data underwent QC, compensation, arcsinh transformation, and normalization.[25,26] Lineage-specific pregating was followed by unsupervised clustering using FlowSOM and ConsensusClusterPlus.[27,28]

Statistical Analysis

Uniform Manifold Approximation and Projection (UMAP) visualizations were generated from all markers with downsampling (≤1,000 cells/sample). Group differences in cluster abundance were tested by limma (age as covariate, BH-FDR <0.05). Analyses were performed in R version 4.2.2.

Data Availability

All relevant data and analyses are provided in the accompanying eFigures and eTables. Additional data sets supporting the conclusions of this study are available from the corresponding author upon reasonable request.

Results

Proteomic Profiling of CSF in MOGAD Compared With MS and AD Using NULISA Platform

To delineate the proteomic signatures underlying MOGAD pathology, we first analyzed CSF protein profiles from patients with MOGAD, MS, and AD using NULISA platform, as shown in Figure 1, the experimental workflow.

CSF MOGAD vs MS

When comparing soluble protein expression in the CSF of MOGAD and MS (collected within 30 days after attack onset), 142 proteins were identified as differentially expressed (Figure 2A, eTables 2 and 3). The proteins elevated in MOGAD largely reflected distinct biological processes. A subset of cytokines and growth factors including IL18, IL36B, CSF3, KITLG, FGF2, PGF, AREG, and PTN, indicated enhanced cytokine and regulation of cell-cell adhesion (Figure 2B). In parallel, proteins linked to oxidative and metabolic stress, such as MPO, NAMPT, PARK7, HBA1, and ENO2, were also increased, suggesting activation of redox and metabolic pathways in MOGAD. Molecules involved in endothelial and myeloid trafficking and tissue remodelling, including LCN2, MMP8, SELE, S100A12, and PTX3, were also upregulated, consistent with peripheral immune activation and CNS recruitment markers. Additional DEPs, such as IKBKG, PDLIM5, TARDBP, VEGFC, VEGFD, YWHAZ, ARSA, and C1QA, were associated with immune signaling and neuroprotective or repair-related responses.

By contrast, proteins enriched in MS compared with MOGAD included TNFRSF13B, IL17B, CCL19, CD40LG, CX3CL1, CD27, IFNG, TNFRSF17, IL12B, and GFAP, highlighting B-cell pathology and immune-mediated inflammation in MS. Pathway enrichment analysis of the 142 DEPs using KEGG 2021 Human and GO 2025 (Biological Process, Cellular Component, and Molecular Function) revealed strong associations with cytokine-mediated signalling, regulation of cell-cell adhesion, and leukocyte and myeloid migration (eFigure 1A). Visualization of molecular function terms highlighted 2 main interaction clusters: one encompassing proinflammatory growth factors, such as IL36B, KITLG, and CSF3, connected to growth factor receptor binding and receptor-ligand activity and another centered on antioxidant and peroxidase functions, driven by HBA1, PARK7, and PRDX6 (eFigure 1B).

CSF MOGAD vs AD

Comparative analysis of CSF protein profiles between MOGAD and AD revealed 118 DEPs (Figure 2C, eTables 4 and 5). The proteins upregulated in MOGAD included several overlapping with those enriched relative to MS, notably IL18, IL1B, IL1RL1, IL24, IL32, IL33, IL36B, CSF3, KITLG, PGF, and PTN, reflecting sustained proinflammatory and growth factor activity in MOGAD compared with AD (Figure 2D). In addition, oxidative stress–related molecules such as MPO, NAMPT, PARK7, PRDX6, and HBA1 were elevated, together with immune signalling components (C1QA, CCL7, CD70, HLA-DRA) and neuroprotective or stress-response proteins (ARSA, REST, RUVBL2, TARDBP, YWHAZ). By contrast, as expected, AD patients displayed higher CSF levels of phosphorylated tau isoforms (pTau-217, pTau-231, pTau-181), as well as TNFRSF13B, IL17B, GFAP, CCL19, CD40LG,

Figure 2 CSF Proteomic Profile in MOGAD Compared With MS and AD

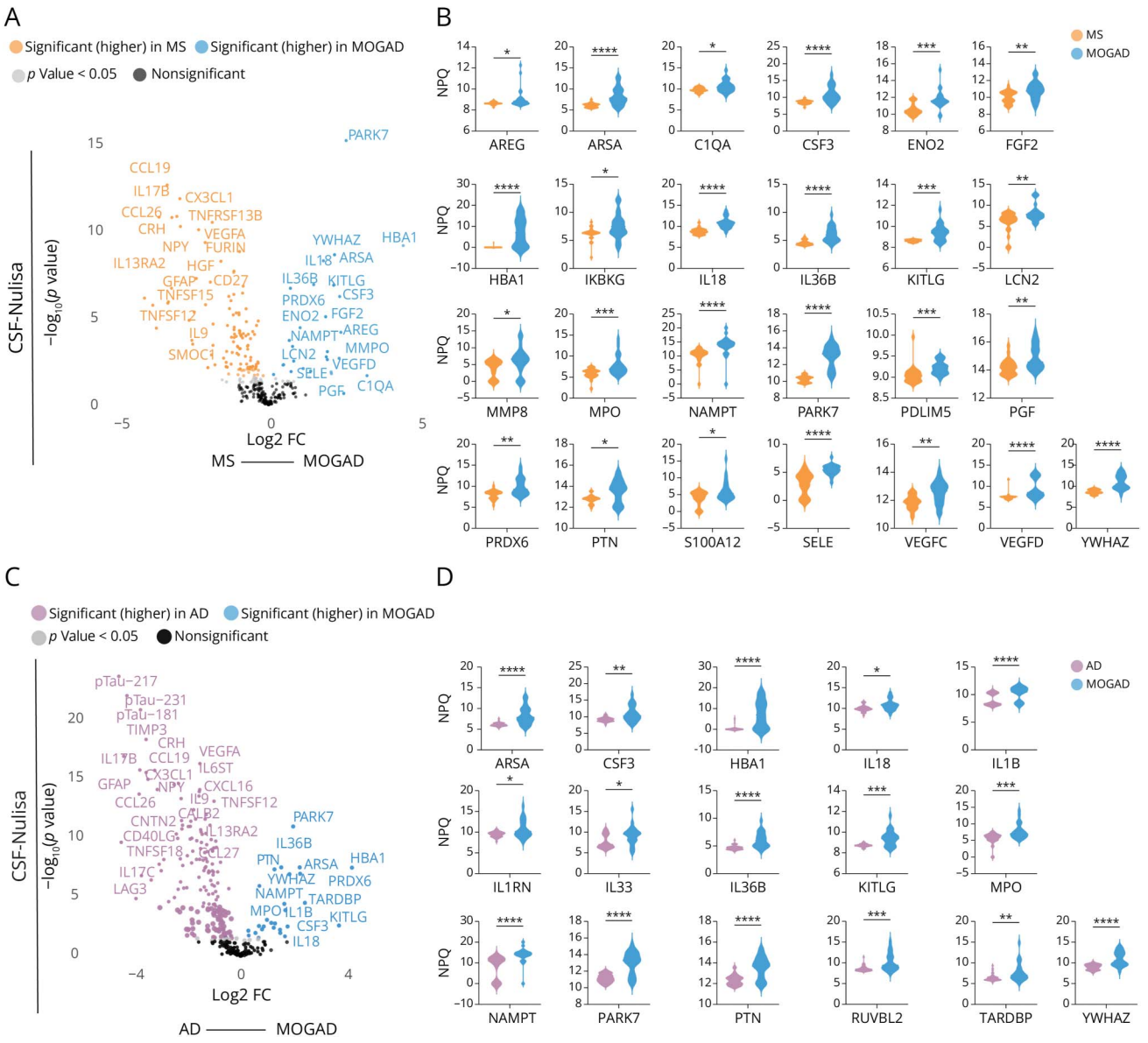

(A) Differentially expressed proteins (DEPs) identified in CSF samples from MOGAD (treatment-naïve, n = 21) and MS (treatment-naïve, n = 22) patients analyzed using the NULISA platform. (B) The volcano plot (left) displays the DEPs, with each dot representing a single protein and the horizontal dashed line indicating the *p* value threshold of 0.05. Highlighted proteins represent DEPs that remained statistically significant after multiple-testing correction using FDR-adjusted *p*-values. For the violin plots, statistical significance was determined using the Mann–Whitney *U* test with adjustment for multiple comparisons using the Benjamini–Krieger–Yekutieli procedure. (C) Differential expression analysis of CSF samples from MOGAD (n = 21) and AD (treatment-naïve, n = 36) patients. (D) The volcano plot (left) displays the DEPs, while the violin plots (right) show the top 25 proteins significantly increased in MOGAD. Highlighted proteins represent DEPs that remained statistically significant after multiple-testing correction using FDR-adjusted *p* values. For the violin plots, statistical significance was determined using the Mann–Whitney *U* test with adjustment for multiple comparisons using the Benjamini-Krieger-Yekutieli procedure. MOGAD = myelin oligodendrocyte glycoprotein antibody-associated disease.

CX3CL1, and TIMP3, consistent with neurodegeneration-associated and astroglial activation patterns.

Notably, ARSA, HBA1, IL36B, MPO, NAMPT, and PRDX6 were consistently elevated in MOGAD when compared with both MS and AD (eFigure 1C). ARSA, a lysosomal sulfatase, may participate in demyelination processes, whereas IL36B, MPO, and NAMPT represent potent proinflammatory mediators. MPO contributes to oxidative stress and has been detected in MS lesions, while extracellular NAMPT functions as a damage-associated molecular pattern linking NAD^+ metabolism with microglial activation and CNS inflammation. PRDX6 and HBA1 further point to the involvement of antioxidant and redox-regulatory mechanisms in MOGAD-associated neuroinflammation.

CSF and Serum Proteomic Profiles Using the Olink Platform (MOGAD vs MS)

Given the NULISA results indicating distinct inflammatory and metabolic signatures in the MOGAD CSF compartment,

we next sought to evaluate whether these processes were conserved across compartments in both MOGAD and MS. To this end, we performed large-scale proteomic profiling of CSF and serum using the Olink Explore 3072 platform.

CSF Olink Profiling

Comparison of CSF protein expression between MOGAD and MS identified 76 DEPs (Figure 3A, eTables 6 and 7). Among these, 22 proteins were significantly elevated in MOGAD (Figure 3B). These CSF DEPs elevated in MOGAD could be grouped into 2 coordinated biological pathways: Inflammatory mediators including IL1A, IL36G, C3, ARG1, ANXA2, APEX1, BDNF, SEMA4C, and WFDC12 reflected activation of CNS innate immune signalling, neuroimmune communication, and glial stress responses. In parallel, a metabolic and vascular remodelling signature comprising COL4A1, AGT, FBP1, BCAT1, PGD, ENO3, IDI2, CA3, AHSP, SERPINA12, and LBR indicated shifts in endothelial integrity, redox buffering, and cellular energy metabolism. Together, these findings confirmed that MOGAD can be characterized by the convergence of CNS inflammatory activation and metabolic-vascular remodelling, reinforcing that disease activity is not restricted to immune activation alone. To assess cross-platform concordance, we compared CSF DEPs identified by NULISA and Olink (eFigure 2). Of the 142 NULISA-derived CSF DEPs, 25 were not represented in the Olink panel. Among the overlapping proteins, 6 (PARK7, FURIN, CD27, TNFRSF17, TIMP3, and BDNF) were also differentially expressed in CSF by Olink.

Serum Olink Profiling

To determine whether CSF proteomic changes were reflected systemically, we next analyzed serum samples. Differential analysis identified 507 DEPs, most of which were elevated in MOGAD (Figure 3C, eTables 8 and 9). Notably, 9 proteins AHCY, ANXA2, APEX1, ARG1, AHSP, BCAT1, LBR, PGD, and SEMA4C were consistently upregulated in both CSF and serum, indicating shared central and peripheral alterations.

Top-ranked serum DEPs elevated in MOGAD grouped into 2 coordinated biological pathways. A cluster of inflammatory mediators, including IL18R1, LTA4H, CTSC, NFKB1, CRELD1, and SUSD2, reflected activation of innate immune signalling and leukocyte interaction networks. In parallel, a cardiometabolic signature comprising APOL1, PCSK9, FABP5, ENO1, MME, FST, and CILP indicated metabolic remodelling and vascular-lipid regulatory processes. Together, these findings support a model in which MOGAD involves both immune-driven inflammation and systemic cardiometabolic adaptation, rather than isolated CNS-restricted pathology (eFigure 3).

High-Dimensional Immune Profiling of Whole-Blood Samples Using CyTOF

To further link systemic protein signatures with immune cell phenotypes, we next performed high-dimensional immune profiling of whole-blood samples from patients with MOGAD and MS using mass cytometry (CyTOF). Three antibody panels targeting major immune cell lineages T cells, B cells, myeloid cells, NK cells, and granulocytes were used, encompassing a total of 123 protein markers (eFigure 4, eTable 10–12 and eFigure 5–7).

Compared with patients with MS, individuals with MOGAD exhibited a lower frequency of naïve $CD4^+$ T cells ($CD4^+CD28^+CD45RO^-CCR7^+$; cluster T1) (Figure 4A, eTable 13) and a modest reduction in transitional B cells ($CD19^+CD24^+CD38^+$; clusters B1 and B3) (Figure 4B), indicating decreased representation of lymphocyte subsets associated with immune regulation and peripheral tolerance (eTable 14). Patients with MS showed an increased proportion of pro-inflammatory classical monocytes ($CD14^+CD33^+CD95^+MIP\text{-}1\beta^+$; cluster M1), whereas patients with MOGAD were enriched for a less activated classical monocyte population ($CD14^+CD33^{low}CD95^{low}MIP\text{-}1\beta^-$; cluster M2) (Figure 4C, eTable 14). Moreover, the monocyte compartment also diverged between the 2 diseases. Patients with MOGAD also demonstrated a reduction in BAFF-expressing activated neutrophils ($CD15^+CD16^+CD86^+CD172a^+BAFF^+$; cluster N1) (Figure 4D), suggesting attenuated granulocyte-mediated immune amplification relative to MOGAD in comparison with patients with MS, as previously described.[17]

This shift toward a less activated circulating myeloid profile in MOGAD, together with the reduced frequencies of naïve $CD4^+$ T cells and transitional B cells, suggests that the heightened inflammatory proteomic signatures observed in MOGAD (by NULISA and Olink) may not result from elevated myeloid activation in the periphery, but rather from reduced regulatory lymphocyte-mediated immune restraint, together with amplified CNS compartment (represented by CSF) cytokine signalling, particularly involving IL-1 family pathways. By contrast, MS is characterized by sustained peripheral myeloid activation and enhanced antigen-presentation programs, consistent with its chronic autoimmune inflammatory profile.[29]

Immuno-Proteomic Signatures Distinguishing Monophasic and Relapsing MOGAD

Given the reduced regulatory lymphocyte representation and elevated inflammatory signalling observed in MOGAD, we next investigate whether these cellular and molecular features differentiate patients with monophasic disease from those who progress to a relapsing course. We performed differential proteomic analysis using the Olink Explore platform, comparing patients with a relapsing course (n = 18) to those with a monophasic course (a single clinical attack since diagnosis; n = 16). Relapsing MOGAD was defined as ≥1 clinical relapse from the earliest documented attack to the most recent follow-up (eTable 15). This analysis identified 119 DEPs distinguishing monophasic and relapsing MOGAD (Figure 5A and eTable 16). Several proteins, including CRELD1, CD2, CASP4, IL10, FH, MATN3, GH2, and IL32, were elevated in monophasic MOGAD, whereas IL13,

Figure 3 CSF and Serum Olink Proteomic Profile in MOGAD Compared With MS

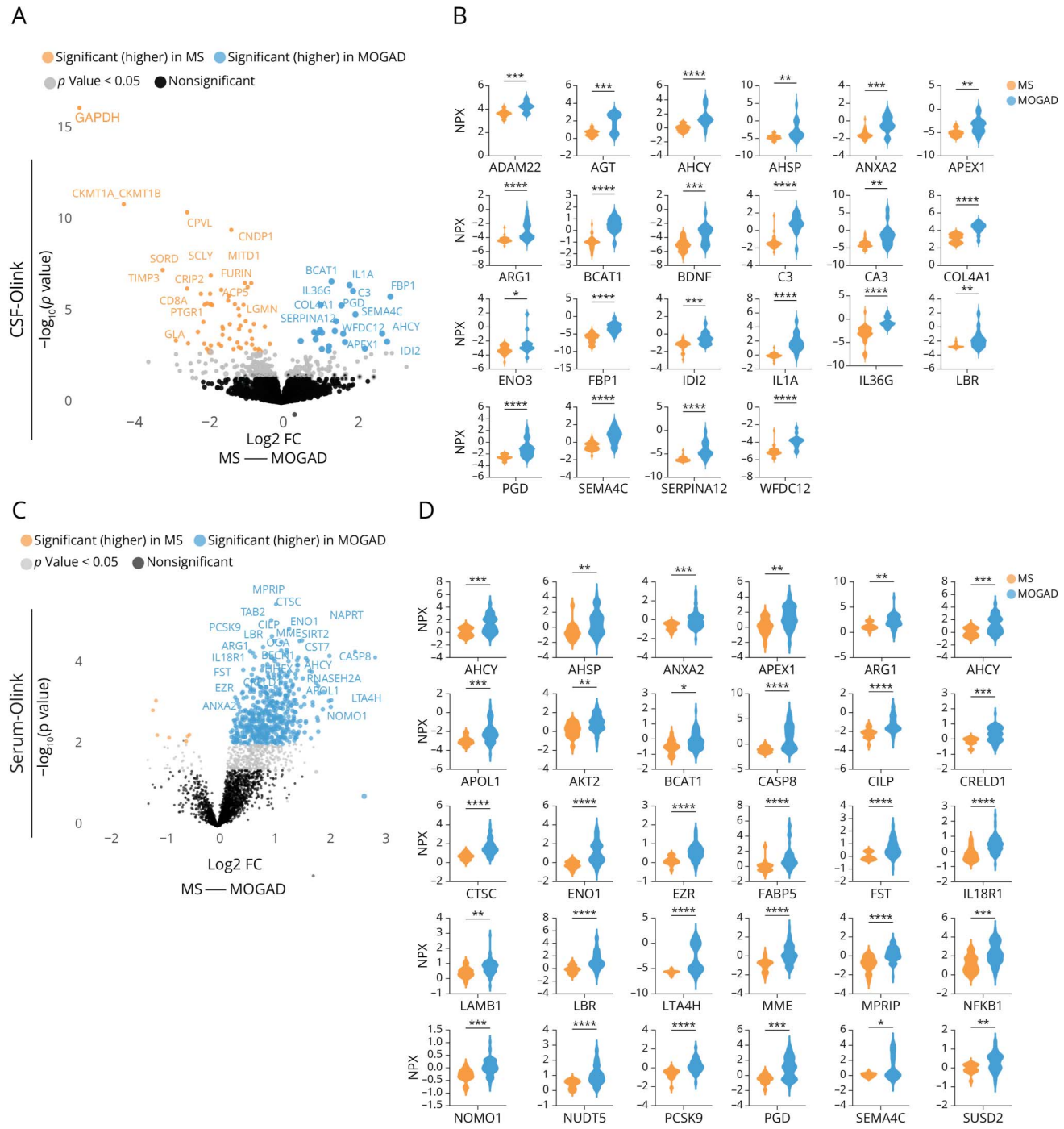

(A) Differentially expressed proteins (DEPs) identified in CSF samples from MOGAD (treatment-naïve, n = 13) and MS (treatment-naïve, n = 28) patients using the Olink Explore platform. These samples were partly overlapped with those analysed with NULISA platform. The volcano plot displays the DEPs, with each dot representing a single protein and the horizontal dashed line indicating the p value threshold of 0.05. Highlighted proteins represent DEPs that are statistically significant after multiple-testing correction based on adjusted p-values (FDR). (B) Violin plots depict the top DEPs with higher expression in MOGAD, identified by Olink (as Olink Normalized protein expression [NPX]) values. (C) Differential expression analysis of Serum samples from MOGAD (n = 65 [14 DMT-treated]) and MS (n = 16 [4 DMT-treated]) patients. The volcano plot displays the DEPs. (D) For the violin plots, statistical significance was determined using the Mann–Whitney U test with adjustment for multiple comparisons using the Benjamini-Krieger-Yekutieli procedure. $p < 0.05$, $^{**}p < 0.01$, $^{***}p < 0.001$, and $^{****}p < 0.0001$. MOGAD = myelin oligodendrocyte glycoprotein antibody-associated disease.

MAP2K6, COPB2, DAPP1, YOD1, and STX8 were increased in relapsing patients. Most DEPs displayed significant correlations with the total number of relapses, while only a minority showed associations with disease duration or age (Figure 5B and eTable 17). Given the limited sample size, these findings should however be considered exploratory and hypothesis-generating, reflecting association trends rather than definitive group-level differences.

Figure 4 Whole Blood Immune Cell Immune Profiling

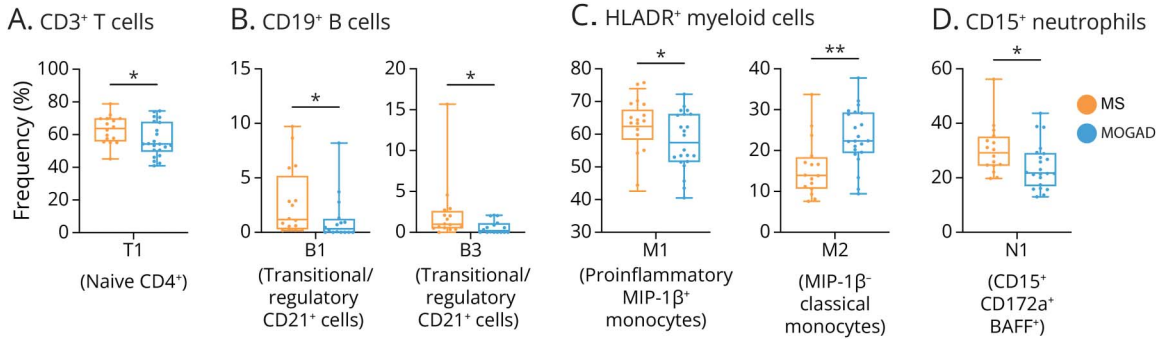

(A) Immune cell populations in whole blood were profiled using CyTOF with 3 antibody panels. (B) The box plots on the right display significantly different cell populations between MS (n = 16 [4 DMT-treated]) and MOGAD (n = 22 [9 DMT-treated]). Each dot represents an individual sample; boxes span the interquartile range (25th–75th percentile), whiskers denote the minimum and maximum values, and the horizontal line indicates the median. Statistical significance was assessed using the Mann–Whitney *U* test without correction for multiple comparisons. MOGAD = myelin oligodendrocyte glycoprotein antibody-associated disease.

Based on these observations of reduced regulatory lymphocyte representation in MOGAD (as shown in Figure 4), we next examined whether variation within the T-cell compartment was associated with clinical disease activity, particularly relapse susceptibility in MOGAD. To this end, we performed a focused analysis of regulatory and memory-associated T-cell subsets, including Tregs and $CD8^+$ RTE-like cells. A total of 12 $CD3^+$ T-cell clusters were identified, of which 2 differed significantly between monophasic and relapsing MOGAD patients: T4 ($CD4^-CD8^-CD57^+TCR\gamma\delta^+$), a proinflammatory double-negative (DN) γδ T cells; and T10 ($CD4^-CD8^+CCR7^+CD31^+CTLA4^+$), a CD31-expressing $CD8^+$ T-cell subset with a phenotype similar to that reported for naïve/RTE-like cells[18,19] (Figure 5C and eTables 18, 19). In relapsing MOGAD, the frequency of $CD4^+CD25^+CD127^{low}ICOS^+CD39^+$ regulatory T cells (T2) was lower compared with monophasic disease; however, this difference did not reach statistical significance and should be interpreted cautiously.

Correlation analysis integrating immune and proteomic data revealed significant associations between immune cell populations, circulating proteins, and clinical parameters, including disease duration, number of relapses (since diagnosis), and patient age (Figure 5D and eTable 20). Interestingly, the T2 cluster correlated positively with CASP4, FGL1, GBP2, IL32 (a cytokine known to stabilize $FOXP3^+$ Treg function), and BEX3, linking these populations with active inflammatory processes. No significant associations were observed between age and the 3 T-cell clusters (Figure 5D). The T10 CD31-expressing cluster exhibited a negative correlation with the total number of relapses ($p < 0.05$), indicating a protective association (Figure 5D). In contrast, the T4 γδ T-cell subset correlated positively with relapse frequency. Protein correlations further supported this pattern: IL13 and CDKL5 were negatively correlated with T10, whereas ANGPTL1, FCER1A, and TSPAN1 correlated positively. The T4 cluster showed positive associations with IL13, while LRGI1, BEX3, FCRL6, IL32, FH, and DEFB1103A/B were inversely correlated.

Immuno-Proteomic Signatures Associated With Optic Neuritis

Clinical phenotypes among patients with MOGAD included optic neuritis (ON, n = 16), myelitis (n = 16), brainstem involvement (n = 5), and cerebral involvement (n = 1); no diencephalic or area postrema presentations were observed (eTable 15). Stratification by clinical phenotype revealed distinct proteomic signatures associated with ON vs non-ON MOGAD (Figure 6A, eTable 21). IL-13 levels were higher in the non-ON group, compared with ON-predominant disease and showed a negative correlation with disability as measured by EDSS, whereas no significant association with EDSS was observed in ON patients (Figure 6B, eTable 22).

For CyTOF analyses, samples from 22 patients were available and stratified into ON-predominant (n = 13) and non-ON (n = 9) subgroups. ON-predominant patients exhibited reduced frequencies of $CD4^+$-naïve T cells (cluster T1) and enrichment of unconventional T-cell subsets, including MAIT-like $CD8^+$ T cells (cluster T6) and a distinct population of double-negative γδ T cells characterized by a $CD57^-CCR5^{hi}CD161^{hi}$ phenotype (cluster T8) (Figure 6C, eTable 23). This γδ T-cell population was phenotypically distinct from the $CD57^+CCR5^-CD161^-$ γδ T-cell subset associated with relapsing MOGAD identified in Figure 5. Notably, in phenotype-stratified analyses, proteomic profiles associated with immune cell candidates differed between ON and non-ON presentations. IL-13 did not correlate with ON-associated immune cell populations, suggesting that its relationship with disability may differ according to clinical presentation (Figure 6D, eTables 24 and 25).

Figure 5 Proteomic Signature Differentiating Monophasic and Relapsing MOGAD

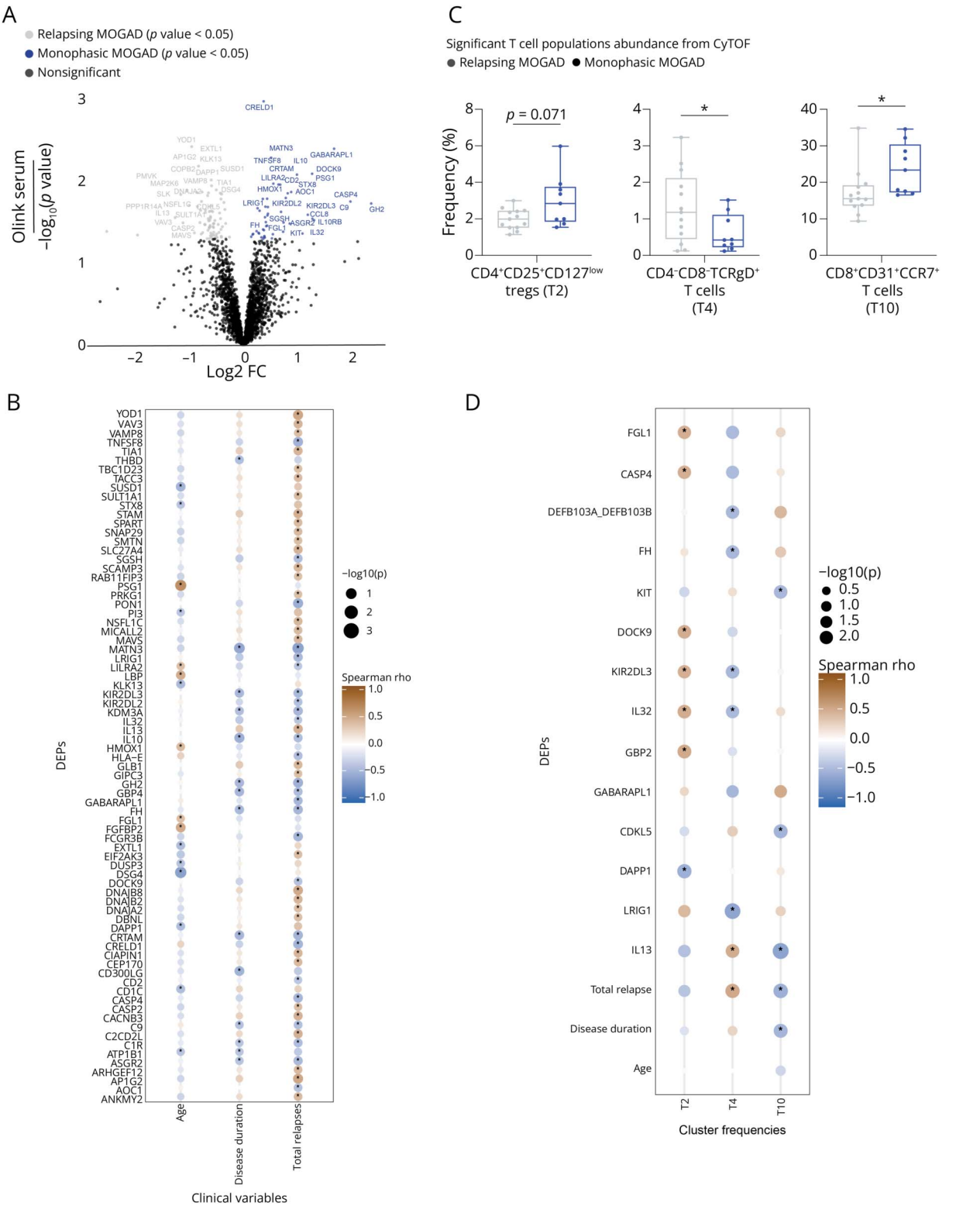

DEPs identified in Serum samples from relapsing MOGAD (n = 18 [7 DMT-treated]) and MOGAD in a monophasic phase (n = 16 [7 DMT-treated]) patients using the Olink Explore platform. All these samples were collected at the remission phases. (A) The volcano plot displays the DEPs, with each dot representing a single protein and the horizontal dashed line indicating the *p* value threshold of 0.05. (B) Spearman correlation analysis between DEPs and clinical variables. (C) The box plots display significantly different cell populations between relapsing MOGAD (gray, n = 12) and MOGAD in monophasic course (blue, n = 10). Each dot represents an individual sample; boxes span the interquartile range (25th–75th percentile), whiskers denote the minimum and maximum values, and the horizontal line indicates the median. Statistical significance was assessed using the Mann–Whitney *U* test. (D) Spearman correlation analysis between DEPs, clinical variables, and identified significant clusters. The bubble plot displays correlation coefficients (Spearman`p). The size of each circle corresponds to the *p* value (raw *p* value < 0.05), with larger circles indicating stronger statistical significance. Color coding reflects the direction of the correlation: brown indicates a positive correlation and blue a negative correlation. MOGAD = myelin oligodendrocyte glycoprotein antibody-associated disease; DEP = differentially expressed protein.

Figure 6 Immune Cell and Proteomic Signatures of MOGAD Patients Stratified by Clinical Phenotype

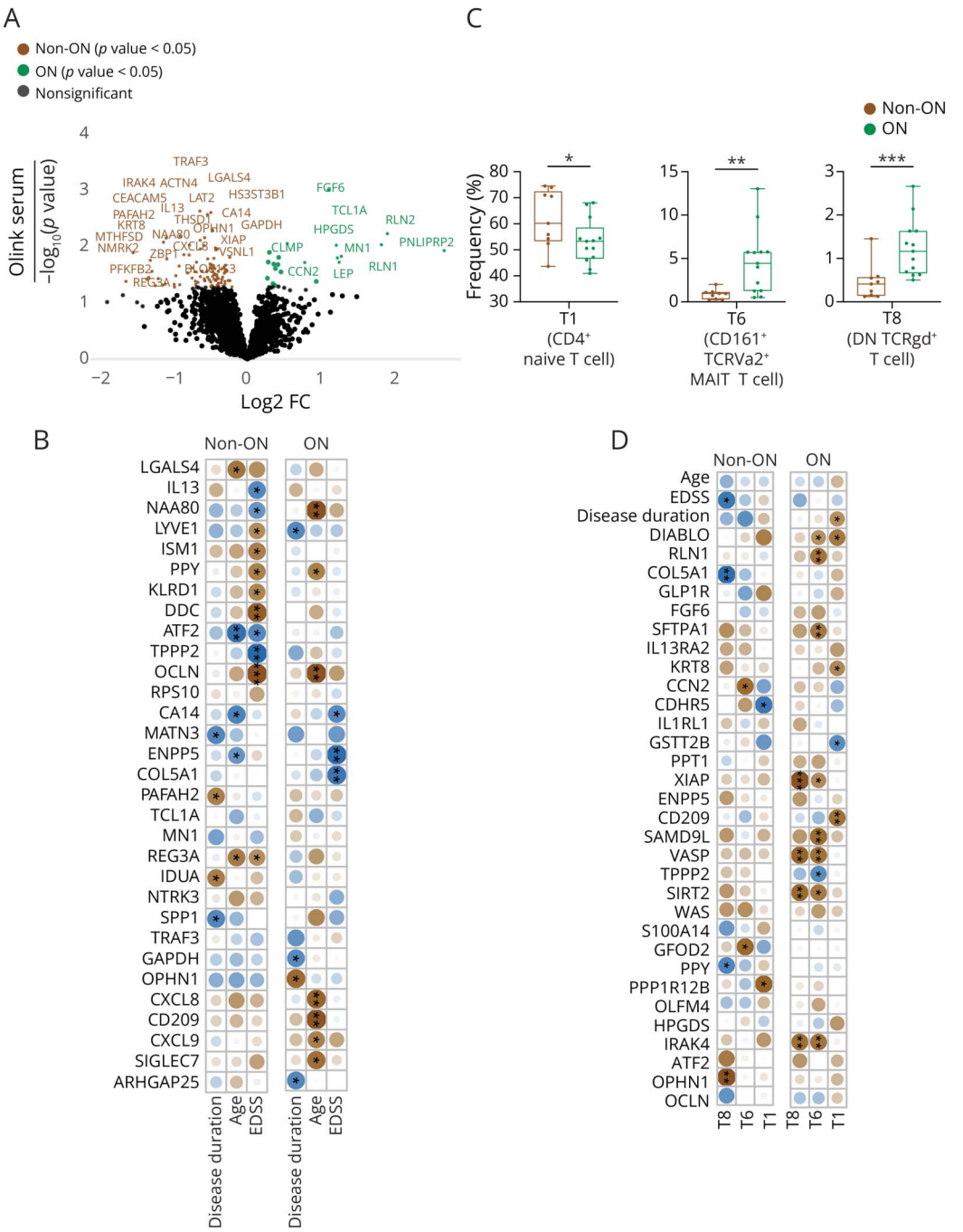

MOGAD patients were stratified into optic neuritis–predominant (ON, green, n = 13)) and non–optic neuritis (non-ON, brown, n = 9) groups. (A) The volcano plot displays the DEPs, with each dot representing a single protein and the horizontal dashed line indicating the *p* value threshold of 0.05. (B) Spearman correlation analysis between DEPs and clinical variables. (C) Box plots show immune cell populations identified by CyTOF that differed significantly between non-ON and ON patients. Each dot represents an individual sample. Boxes indicate the interquartile range (25th–75th percentile), whiskers represent the minimum and maximum values, and the horizontal line denotes the median. Statistical significance was assessed using the Mann–Whitney *U* test (not corrected for multiple comparisons). **p* < 0.05, ***p* < 0.01, ****p* < 0.001. (D) Spearman correlation analysis of differentially abundant clusters and DEPs. Bubble size corresponds to statistical significance (raw *p* < 0.05), with larger circles indicating stronger significance. Color indicates correlation direction (brown, positive; blue, negative). MOGAD = myelin oligodendrocyte glycoprotein antibody-associated disease; DEP = differentially expressed protein.

Discussion

In this integrative immune-proteomic study, we identified molecular and cellular patterns that distinguish MOGAD from MS-associated neuroinflammation and neurodegeneration-associated inflammation in AD. Cross-compartment proteomic profiling revealed coordinated inflammatory and cardiometabolic signals across CSF and blood in MOGAD, consistent with the presence of a systemic immune-metabolic component rather than an exclusively CNS-restricted process. These profiles differed

from MS, which showed greater enrichment of antigen-presentation and costimulatory pathways, and from AD, where neurodegeneration-associated markers predominated. At the cellular level, MOGAD was associated with reduced frequencies of naïve $CD4^+$ T cells and transitional B cells, subsets linked to immune homeostasis. Together, these observations are consistent with MOGAD exhibiting immune features that differ from both MS and AD and suggest that alterations in regulatory immune composition may be relevant to disease biology.

Recent high-parametric spectral flow cytometry analyses by Schmid et al.[30] provide complementary insight into MOGAD immunopathology, highlighting selective reductions in circulating $CXCR3^+CD4^+$ central memory T cells, interpreted as reflecting altered immune cell trafficking and extrafollicular B-cell activation. Our findings are broadly aligned with this framework but suggest an additional layer of immune dysregulation, characterized by reduced naïve $CD4^+$ T cells, transitional B cells, and BAFF-expressing neutrophils. Methodological differences likely contribute to the partially distinct cellular compartments emphasized, as spectral flow cytometry focused on detailed lymphoid phenotyping, whereas our CyTOF panels enabled broader simultaneous assessment of lymphoid, myeloid, and granulocyte populations integrated with NULISA and Olink proteomic analyses. Taken together, these studies are compatible with a model in which MOGAD involves both altered immune cell trafficking and changes in regulatory immune balance.

Patients with MOGAD also showed reduced frequencies of BAFF-expressing activated neutrophils ($CD15^+CD16^+CD86^+CD172a^+BAFF^+$), consistent with reports of lower neutrophil activation and degranulation signatures in MOGAD compared with MS.[31,32] Elevated neutrophil-derived markers such as MPO, NGAL, and MMP-8/9 are well established in MS and contribute to blood–brain barrier disruption and inflammatory tissue injury.[31] By contrast, emerging evidence suggests a more restrained or heterogeneous granulocytic response in MOGAD, with BAFF potentially exerting context-dependent immunomodulatory effects.[17] These observations are consistent with reduced systemic granulocyte-mediated inflammatory amplification in MOGAD relative to MS and may contribute to the distinct inflammatory profiles observed across diseases.

Within MOGAD, relapsing disease was associated with expansion of specific double-negative (DN) γδ T-cell populations and distinct proteomic patterns. IL-13 levels were higher in relapsing MOGAD and correlated positively with relapse frequency, whereas IL-32 and CASP4 showed inverse relationships and were positively associated with regulatory T-cell abundance. IL-13 also displayed an inverse association with $CD8^+CCR7^+CD31^+CTLA4^+$ cells, while this subset correlated positively with ANGPTL1 and CLEC4A, suggesting potential links between regulatory T-cell–associated states and tolerogenic protein networks. These associations do not establish causality but point toward coordinated immune–proteomic relationships that may differ between disease courses.

In phenotype-stratified analyses, IL-13 was increased in non–optic neuritis (non-ON) presentations and showed an inverse association with disability, but did not correlate with ON-associated immune cell populations. This pattern suggests that IL-13 may be linked to distinct immunologic contexts depending on clinical presentation. Together with relapse-associated findings, these data indicate that IL-13 may participate in heterogeneous immune processes in MOGAD, associating with relapse susceptibility at the disease-course level while showing an inverse relationship with disability in non-ON phenotypes. EDSS correlation analyses further suggested phenotype-dependent proteomic patterns, with several relapse-associated proteins correlating with disability in non-ON presentations but not in ON-predominant disease, whereas ON-associated signatures showed limited or divergent associations with EDSS. Although exploratory given cohort size, these findings are consistent with the notion that molecular correlates of disease activity and disability in MOGAD may vary by clinical phenotype.

Our analyses further identified 2 phenotypically distinct DN γδ T-cell populations associated with different clinical contexts in MOGAD. A $CD57^+CCR5^-CD161^-$ DN γδ T-cell subset was linked to relapsing disease, whereas ON-predominant patients showed enrichment of a separate $CD57^-CCR5^{hi}CD161^{hi}$ DN γδ T-cell population. This heterogeneity suggests that DN γδ T cells may reflect different immune activation states related to disease course vs clinical phenotype rather than a uniform pathogenic population. Given the exploratory nature of these findings and the limited cohort size, additional functional and longitudinal studies will be required to clarify whether these DN γδ T-cell subsets have distinct roles in relapse susceptibility or tissue-specific inflammation.

RTEs decline with age and contribute to peripheral immune tolerance both directly and as precursors of the adult Treg pool.[18,19] We observed reduced frequencies of CD31-expressing RTE-like $CD8^+$ T cells in relapsing MOGAD, raising the possibility that altered thymic output or peripheral maintenance of regulatory lineages may be associated with relapse susceptibility. However, owing to the absence of functional assays and limitations of the CyTOF marker panels, the regulatory function and precise origin of this $CD8^+$ subset cannot be confirmed, as CD31 can also be expressed by memory-like $CD8^+$ T cells.[19,33,34] Supporting the presence of altered regulatory balance, IL-32—previously implicated in stabilization of $FOXP3^+$ Treg function—was reduced in relapsing MOGAD and correlated positively with Treg abundance.[35] Collectively, these observations are compatible with a model in which relapse susceptibility in MOGAD reflects

reduced regulatory resilience rather than sustained peripheral inflammatory activation.

From a translational perspective, the immune-proteomic patterns identified here may inform future efforts toward risk stratification and disease monitoring. While MOG-IgG seropositivity is central for diagnosis, its prognostic value for relapse risk is limited. Integrating circulating molecular data with regulatory lymphocyte frequencies and relapse-associated proteins such as IL-13, IL-32, CASP4, ANGPTL1, and PTN highlights candidate pathways that warrant further investigation in longitudinal and functional studies. Such biomarker-based stratification may become increasingly relevant given the evolving therapeutic landscape and interest in early preventive treatment in MOGAD.

Several limitations should be considered. Subgroup analyses were constrained by cohort size and relapse frequency distribution, and longitudinal sampling remains limited. The immune signatures identified by CyTOF should be regarded as exploratory and require confirmation using expanded antibody panels, including markers such as FOXP3 for regulatory T-cell characterization and more definitive RTE markers, as well as validation in larger, independent cohorts. In addition, a subset of shared proteins showed discordant direction or magnitude of change across platforms (e.g., PARK7, FURIN, BDNF), likely reflecting technical differences in antibody pairs, epitope recognition, assay sensitivity, and dynamic range that are known to affect cross-platform concordance in targeted proteomics.

Classification into relapsing vs monophasic MOGAD was based on clinical course at the time of sampling and may partially reflect cumulative attack burden rather than fixed disease-course biology, as some patients classified as monophasic may experience subsequent relapses. Consistent with International MOGAD Panel data indicating a median time to first relapse of approximately 11 months, this represents an inherent limitation of cross-sectional analyses. To mitigate this, we incorporated total attack counts across longitudinal follow-up and interpret the observed immune–proteomic associations as descriptive and hypothesis-generating rather than predictive.

Finally, although most patients were not receiving disease-modifying treatment (DMT) at the time of sampling, a subset had prior DMT exposure with an adequate washout period. While the absence of active treatment reduces the likelihood that the observed immune-proteomic profiles reflect direct pharmacologic effects, prior therapy cannot be fully excluded as a potential confounder. This limitation is intrinsic to cross-sectional studies in rare diseases and should be considered when interpreting these findings.

MOGAD is associated with immune-proteomic patterns that differ from those observed in MS and AD and that vary according to disease course and clinical phenotype. Relapsing MOGAD is characterized by alterations in regulatory lymphocyte-associated signatures and corresponding proteomic patterns, consistent with impaired peripheral immune regulation. These findings generate testable hypotheses regarding relapse biology and provide a framework for future longitudinal and functional studies aimed at refining biomarker-based monitoring and therapeutic strategies in MOGAD.

Acknowledgment

The authors thank the BERLimmun team at the Charité - Universitätsmedizin Berlin, the Neurology Unit of the University of Verona (Italy) and Department of Neurology at Ruhr University Bochum for the collection of biospecimens, biobanking and meta and clinical data. The authors acknowledge the assistance of the BIH Cytometry Core Facility, especially to Dr. Leona Simon (BIH at Charité - Universitätsmedizin Berlin, Germany). This study was in part funded by F. Hoffmann-La Roche Ltd as part of Integrative Neuroscience Collaborations Network (INTONATE, MOGAD-Precision, F.P.). The Deutsche Forschungsgemeinschaft (DFG, the German Research Foundation - Project-ID 259373024 - CRC/TRR 167 (B05) (C.B. and C.O.).

Author Contributions

G. Gallaccio: drafting/revision of the manuscript for content, including medical writing for content; major role in the acquisition of data; analysis or interpretation of data. A. Müller: drafting/revision of the manuscript for content, including medical writing for content; analysis or interpretation of data. M. Wang: major role in the acquisition of data; analysis or interpretation of data. L.-M. Diekmann: major role in the acquisition of data; analysis or interpretation of data. C. Otto: analysis or interpretation of data. A. Dinoto: major role in the acquisition of data. V. Chiodega: major role in the acquisition of data. C. Schwake: major role in the acquisition of data. S. Jarius: drafting/revision of the manuscript for content, including medical writing for content; analysis or interpretation of data. T. Usnich: major role in the acquisition of data; analysis or interpretation of data. P.S. Sperber: analysis or interpretation of data. L. Anderhalten: major role in the acquisition of data. T. Ongphichetmetha: drafting/revision of the manuscript for content, including medical writing for content; analysis or interpretation of data. A. Byars: drafting/revision of the manuscript for content, including medical writing for content; analysis or interpretation of data. D. Subasic: drafting/revision of the manuscript for content, including medical writing for content; analysis or interpretation of data. D. Kunkel: major role in the acquisition of data; analysis or interpretation of data. I. Ayzenberg: drafting/revision of the manuscript for content, including medical writing for content; major role in the acquisition of data. S. Mariotto: drafting/revision of the manuscript for content, including medical writing for content; major role in the acquisition of data; analysis or interpretation of data. S. Samadzadeh: drafting/revision of the manuscript for content, including medical writing for content; study concept or

design; analysis or interpretation of data. F. Paul: drafting/revision of the manuscript for content, including medical writing for content; study concept or design; analysis or interpretation of data. C. Böttcher: drafting/revision of the manuscript for content, including medical writing for content; major role in the acquisition of data; study concept or design; analysis or interpretation of data.

Study Funding

INTONATE, MOGAD-Precision by F. Hoffmann-La Roche Ltd.

Disclosure

F. Paul received research support from F. Hoffmann-La Roche Ltd., Alexion Pharma Germany GmbH and Horizon Therapeutics Ireland DAC. Go to Neurology.org/NN for full disclosures.

Publication History

Received by *Neurology® Neuroimmunology & Neuroinflammation* December 4, 2025. Accepted in final form April 22, 2026. Submitted and externally peer reviewed. The handling editor was Associate Editor Romana Höftberger, MD.

References

1. Banwell B, Bennett JL, Marignier R, et al. Diagnosis of myelin oligodendrocyte glycoprotein antibody-associated disease: International MOGAD panel proposed criteria. *Lancet Neurol*. 2023;22(3):268-282. doi:10.1016/s1474-4422(22)00431-8
2. Jarius S, Paul F, Weinshenker BG, Levy M, Kim HJ, Wildemann B. Neuromyelitis optica. *Nat Rev Dis Primers*. 2020;6(1):85. doi:10.1038/s41572-020-0214-9
3. Uzawa A, Oertel FC, Mori M, Paul F, Kuwabara S. NMOSD and MOGAD: an evolving disease spectrum. *Nat Rev Neurol*. 2024;20(10):602-619. doi:10.1038/s41582-024-01014-1
4. Montalban X, Lebrun-Frénay C, Oh J, et al. Diagnosis of multiple sclerosis: 2024 revisions of the McDonald criteria. *Lancet Neurol*. 2025;24(10):850-865. doi:10.1016/s1474-4422(25)00270-4
5. Camera V, Messina S, Tamanti A, et al. Investigating the presence of neurodegeneration independent of relapses in MOGAD compared to relapsing-remitting multiple sclerosis. *Neurol Open Access*. 2025;1(2):e000013. doi:10.1212/wn9.0000000000000013
6. Levy M, Molazadeh N, Bilodeau PA, et al. Multiple types of relapses in MOG antibody disease. *Mult Scler Relat Disord*. 2023;72:104613. doi:10.1016/j.msard.2023.104613
7. Palace J. MOGAD features and outcomes. *J Neurol Sci*. 2023;455:120885. doi:10.1016/j.jns.2023.120885
8. Molazadeh N, Bilodeau PA, Salky R, et al. Predictors of relapsing disease course following index event in myelin oligodendrocyte glycoprotein antibody-associated disease (MOGAD). *J Neurol Sci*. 2024;458:122909. doi:10.1016/j.jns.2024.122909
9. Kim H, Lee EJ, Kim S, et al. Serum biomarkers in myelin oligodendrocyte glycoprotein antibody-associated disease. *Neurol Neuroimmunol Neuroinflamm*. 2020;7(3):e708. doi:10.1212/nxi.0000000000000708
10. Gomes A, Kim SH, Pretzsch R, et al. Neurofilament light chain as a discriminator of disease activity status in MOG antibody-associated disease. *Neurol Neuroimmunol Neuroinflamm*. 2025;12(1):e200347. doi:10.1212/NXI.0000000000200347
11. Gastaldi M, Foiadelli T, Greco G, et al. Prognostic relevance of quantitative and longitudinal MOG antibody testing in patients with MOGAD: a multicentre retrospective study. *J Neurol Neurosurg Psychiatry*. 2023;94(3):201-210. doi:10.1136/jnnp-2022-330237
12. Waters P, Fadda G, Woodhall M, et al. Serial anti-myelin oligodendrocyte glycoprotein antibody analyses and outcomes in children with demyelinating syndromes. *JAMA Neurol*. 2020;77(1):82-93. doi:10.1001/jamaneurol.2019.2940
13. Yandamuri SS, Filipek B, Obaid AH, et al. MOGAD patient autoantibodies induce complement, phagocytosis, and cellular cytotoxicity. *JCI Insight*. 2023;8(11):e165373. doi:10.1172/jci.insight.165373
14. Gawde S, Siebert N, Ruprecht K, et al. Serum proteomics distinguish subtypes of NMO spectrum disorder and MOG Antibody-associated disease and highlight effects of B-cell depletion. *Neurol Neuroimmunol Neuroinflamm*. 2024;11(4):e200268. doi:10.1212/nxi.0000000000200268
15. Zhang C, Zhang TX, Liu Y, et al. B-cell compartmental features and molecular basis for therapy in autoimmune disease. *Neurol Neuroimmunol Neuroinflamm*. 2021;8(6):e1070. doi:10.1212/NXI.0000000000001070
16. Liu J, Yang X, Pan J, et al. Single-cell transcriptome profiling unravels distinct peripheral blood immune cell signatures of RRMS and MOG antibody-associated disease. *Front Neurol*. 2022;12:807646. doi:10.3389/fneur.2021.807646
17. Villacieros-Álvarez J, Espejo C, Arrambide G, et al. Profile and usefulness of serum cytokines to predict prognosis in myelin oligodendrocyte glycoprotein antibody-associated disease. *Neurol Neuroimmunol Neuroinflamm*. 2025;12(3):e200401. doi:10.1212/nxi.0000000000200401
18. Cunningham CA, Helm EY, Fink PJ. Reinterpreting recent thymic emigrant function: defective or adaptive? *Curr Opin Immunol*. 2018;51:1-6. doi:10.1016/j.coi.2017.12.006
19. Bohacova P, Terekhova M, Tsurinov P, et al. Multidimensional profiling of human T cells reveals high CD38 expression, marking recent thymic emigrants and age-related naive T cell remodeling. *Immunity*. 2024;57(10):2362-2379.e10. doi:10.1016/j.immuni.2024.08.019
20. Jack CR, Jr., Bennett DA, Blennow K, et al. NIA-AA research framework: toward a biological definition of Alzheimer's disease. *Alzheimers Dement*. 2018;14(4):535-562. doi:10.1016/j.jalz.2018.02.018
21. Ritchie ME, Phipson B, Wu D, et al. Limma powers differential expression analyses for RNA-sequencing and microarray studies. *Nucleic Acids Res*. 2015;43(7):e47. doi:10.1093/nar/gkv007
22. Nevola Kea. *OlinkAnalyze: Facilitate Analysis of Proteomic Data from Olink. R Package: Olink Proteomics*; 2023. doi:10.32614/CRAN.package.OlinkAnalyze
23. Wang M, Otto C, Fernández Zapata C, et al. Comprehensive analysis of B cell repopulation in ocrelizumab-treated patients with multiple sclerosis by mass cytometry and proteomics. *iScience*. 2025;28(5):112383. doi:10.1016/j.isci.2025.112383
24. Wang M, Dehlinger A, Zapata CF, et al. Associations of myeloid cells with cellular and humoral responses following vaccinations in patients with neuroimmunological diseases. *Nat Commun*. 2023;14(1):7728. doi:10.1038/s41467-023-43553-z
25. Nowicka M, Krieg C, Crowell HL, et al. CyTOF workflow: differential discovery in high-throughput high-dimensional cytometry datasets. *F1000Res*. 2019;6:748. doi:10.12688/f1000research.11622.4
26. Schuyler RP, Jackson C, Garcia-Perez JE, et al. Minimizing batch effects in mass cytometry data. *Front Immunol*. 2019;10:2367. doi:10.3389/fimmu.2019.02367
27. Van Gassen S, Callebaut B, Van Helden MJ, et al. FlowSOM: using self-organizing maps for visualization and interpretation of cytometry data. *Cytometry Part A*. 2015;87(7):636-645. doi:10.1002/cyto.a.22625
28. Wilkerson MD, Hayes DN. ConsensusClusterPlus: a class discovery tool with confidence assessments and item tracking. *Bioinformatics*. 2010;26(12):1572-1573. doi:10.1093/bioinformatics/btq170
29. Haase S, Linker RA. Inflammation in multiple sclerosis. *Ther Adv Neurol Disord*. 2021;14:17562864211007687. doi:10.1177/17562864211007687
30. Schmid J, Alberti C, Power L, et al. Immune signatures link myelin oligodendrocyte glycoprotein antibody-associated disease to other autoantibody-mediated conditions. *Sci Transl Med*. 2025;17(819):eadw0358. doi:10.1126/scitranslmed.adw0358
31. Furlan R, Schaedelin S, Frederiksen JL, et al. Granulocyte and astrocyte markers distinguish MOG-antibody disease and neuromyelitis optica from multiple sclerosis. *Brain*. 2026;149(4):1319-1331. doi:10.1093/brain/awaf345
32. Wang Y, Danzeng Q, Jiang W, et al. A retrospective study of myelin oligodendrocyte glycoprotein antibody-associated disease from a clinical laboratory perspective. *Front Neurol*. 2023;14:1187824. doi:10.3389/fneur.2023.1187824
33. Tanaskovic S, Fernandez S, Price P, Lee S, French MA. CD31 (PECAM-1) is a marker of recent thymic emigrants among CD4+ T-cells, but not CD8+ T-cells or gamma-delta T-cells, in HIV patients responding to ART. *Immunol Cell Biol*. 2010;88(3):321-327. doi:10.1038/icb.2009.108
34. Douaisi M, Resop RS, Nagasawa M, et al. CD31, a valuable marker to identify early and late stages of T cell differentiation in the human thymus. *J Immunol*. 2017;198(6):2310-2319. doi:10.4049/jimmunol.1500350
35. Han L, Chen S, Chen Z, Zhou B, Zheng Y, Shen L. Interleukin 32 promotes Foxp3(+) Treg cell development and CD8(+) T cell function in human esophageal squamous cell carcinoma microenvironment. *Front Cell Dev Biol*. 2021;9:704853. doi:10.3389/fcell.2021.704853